PAPER

Morphology and chirality controlled self-assembled nanostructures of porphyrin–pentapeptide conjugate: effect of the peptide secondary conformation†

Quanbo Wang,[b] Yanli Chen,[c] Pan Ma,[b] Jitao Lu,[b] Xiaomei Zhang*[b] and Jianzhuang Jiang*[a]

An optically active porphyrin–pentapeptide conjugate **1**, actually a porphyrinato zinc complex covalently linked with a glycinyl–alanyl–glycinyl–alanyl–glycine (GAGAG) peptide chain, was designed and synthesized. The self-assembly properties of this novel porphyrin–pentapeptide conjugate in THF/*n*-hexane and THF/water were comparatively investigated by electronic absorption, circular dichroism (CD), IR spectroscopy, transmission electron microscopy (TEM), scanning electron microscopy (SEM), and X-ray diffraction (XRD) technique. Associated with the different secondary conformation of the pentapeptide chain covalently linked to the porphyrin ring in different solvent systems, self-assembly of conjugate **1** leads to the formation of nanofibers with *right*-handed helical arrangement and nanotubes with *left*-handed helical arrangement in a stack of porphyrin chromophores according to the CD spectroscopic result in apolar THF/*n*-hexane (1 : 3) and polar THF/water (1 : 3) system depending on the cooperation between intramolecular or intermolecular hydrogen bonding interaction with chiral discrimination between pentapeptide chains and porphyrin–porphyrin interactions in the direction parallel to the tetrapyrrole ring of neighboring conjugate molecules. IR spectroscopic result clearly reveals the *α*-helix and *β*-sheet secondary conformation, respectively, employed by the pentapeptide chain attached at the porphyrin core in the nanostructures formed in THF/*n*-hexane (1 : 3) and THF/water (1 : 3). The X-ray diffraction (XRD) result confirms that in the nanotubes, a dimeric supramolecular bilayer structure was formed through an intermolecular hydrogen bonding interaction between two conjugate molecules which, as the building block, self-assembles into the target nanostructures. These results clearly reveal the effect of a secondary conformation of pentapeptide chain in the conjugate molecule on the packing mode of porphyrin chromophore, supramolecular chirality, and morphology of the self-assembled nanostructure. The present result represents not only the first example of organic nanostructures self-assembled from a covalently linked porphyrin–pentapeptide conjugate, but more importantly the first effort towards controlling and tuning the morphology and in particular the supramolecular chirality of porphyrin nanostructures *via* tuning the secondary conformation of peptides in different solvent systems, which is helpful towards understanding, designing, preparing, and mimicking the structure and role of naturally occurring porphyrin–peptide conjugates. In addition, both nanofibers and nanotubes were revealed to show good semiconducting properties.

Introduction

Precise and elegant arrangement of peptide-containing porphyrin conjugate systems is very important for the purpose of

conducting corresponding biological reactions in nature.[1] For example, in the light-harvesting complex II of *Rhodopseudomonas acidophila*, the peptides act as templates and optimize the orientation of porphyrins with a ring-shaped geometry, in which effective energy transfer occurs.[2] In *cytochrome c*, proteins provide special sites for ligation to their covalently linked multiple porphyrins (*heme*) to realize corresponding functions such as electron transfer, oxygen transport, NO sensing, oxidant detoxification, and O$_2$ activation.[3] Inspired by the elegance of these naturally occurring supramolecular structures, aggregation behavior of peptide-containing porphyrin systems has attracted extensive research interest for the purpose

[a]Department of Chemistry, University of Science and Technology Beijing, Beijing, 100083, P. R. China. E-mail: jianzhuang@ustb.edu.cn; Fax: (+86) 10-6233-2462

[b]Department of Chemistry, Shandong University, Jinan, 250100, P. R. China. E-mail: zhangxiaomei@sdu.edu.cn; Fax: (+86) 531-8856-5211

[c]Department of Chemistry, University of Jinan, Jinan, 250022, P. R. China

† Electronic supplementary information (ESI) available. See DOI: 10.1039/c1jm10547g

of mimicking the structure and role of natural porphyrin systems in the past decades.[4,5]

Investigation reveals that naturally occurring porphyrins usually exist as either the hybrids with peptide formed depending on electrostatic, hydrogen bonding, and metal–ligand coordination bonding interactions or the conjugates with peptides covalently linked at the porphyrin peripheral positions.[6] As yet, the self-assemble property of porphyrin hybrids with synthetic peptides depending on non-covalently interactions has been extensively studied.[4] However, it seems quite hard to effectively control the excitonic interactions between the light-absorbing porphyrin chromophores in these non-covalently linked self-assembled systems, which are relatively weak due to the limited porphyrin binding sites with peptides[7] and/or the longer distance between porphyrin binding sites than those required for efficient excitonic interactions.[8] In addition to these porphyrin–peptide hybrids, the self-assemble behavior of porphyrin conjugate covalently linked with synthetic peptide was also started to be investigated.[5] However, attention in this direction appears to be focused on their aggregation behavior in solution instead of on the solid state nanostructures.

In the present paper, we describe the design and synthesis of a covalently linked optically active porphyrin–pentapeptide conjugate **1**, actually a porphyrinato zinc complex attached with a glycinyl–alanyl–glycinyl–alanyl–glycine (GAGAG) peptide chain at the *meso*-attached phenyl group, Scheme 1. The self-assembly behavior of this porphyrin–pentapeptide conjugate in different solvent systems was comparatively investigated, revealing the effect of the secondary conformation of the pentapeptide chain covalently linked to the porphyrin ring in the conjugate molecule associated with solvent system on the packing mode of porphyrin chromophore, supramolecular chirality, and morphology of the self-assembled nanostructures. The present result represents not only the first example of organic nanostructures self-assembled from covalently linked porphyrin–pentapeptide conjugate but more importantly the first effort towards controlling the morphology and supramolecular chirality of porphyrin nanostructures *via* tuning the secondary conformation of peptide. This should be helpful towards understanding, designing, preparing, and mimicking the structure and role of naturally occurring porphyrin–peptide conjugate systems.

Results and discussion

Molecular design, synthesis, and characterization

Precise control of supramolecular architecture is a great challenge in the field of molecular self-assembly. The major driving force operating in these precisely controlled nanoscopic architectures arises from the interplay of hydrogen bonding, π–π stacking, electrostatic interactions, steric effects, hydrophobic interactions, and crystallization along with the involvement of growth kinetics. As a result, comprehensive understanding of the interplay among these factors to create different morphologies has formed the focus of current research interests in this field. Porphyrins are of typical large conjugated molecular electronic structure with intrinsic intermolecular π–π interaction.[9] Tuning the intermolecular interaction of such kind of tetrapyrrole derivatives can be easily reached by introducing functional groups (actually additional non-covalent interactions) onto the peripheral positions of porphyrin ring.[10] On the other hand, peptides are well known for their hydrogen bond-forming ability and solvent-dependent secondary conformation nature.[11] As a result, integration of peptide chains with porphyrin chromophores is expected to provide a good chance to tune the optical and electronic properties of porphyrin self-assembled nanostructures on the basis of tuning the molecular packing mode depending on the interplay of π–π interactions between porphyrin chromophores and the hydrogen bonding interaction between peptide chains. In the present case, a simple peptide, namely glycinyl–alanyl–glycinyl–alanyl–glycine (GAGAG) amine-terminated peptide chain with AlaGly motif, was selected to be integrated with a porphyrinato zinc complex.

The target porphyrin–pentapeptide conjugate **1** was synthesized in good yield from the reaction between 5-(4-carboxylphenyl)–10,15,20-tris(4-*tert*-butylphenyl)porphyrinato zinc compound Zn[T(COOH)PP] and a GAGAG peptide in the presence of N,N-diisopropyl ethylamine (DIPEA) and o-benzotriazole-N,N,N′,N′-tetramethyl-uronium-hexafluorophosphate (HBTU) in N,N-dimethylformamide, Scheme 1. A satisfactory elemental analysis result was obtained for this newly prepared conjugate after repeat column chromatography and recrystallization. The MALDI-TOF mass spectrum of the compound clearly showed an intense signal for the molecular ion [M]+. The isotopic pattern closely resembles the simulated one given in

ZnT(COOH)PP   **GAGAG-NH₂**   **1**

HBTU = o-Benzotriazole-N,N,N′,N′-tetramethyl-uronium-hexafluorophosphate
DIPEA = N,N-Diisopropyl ethylamine
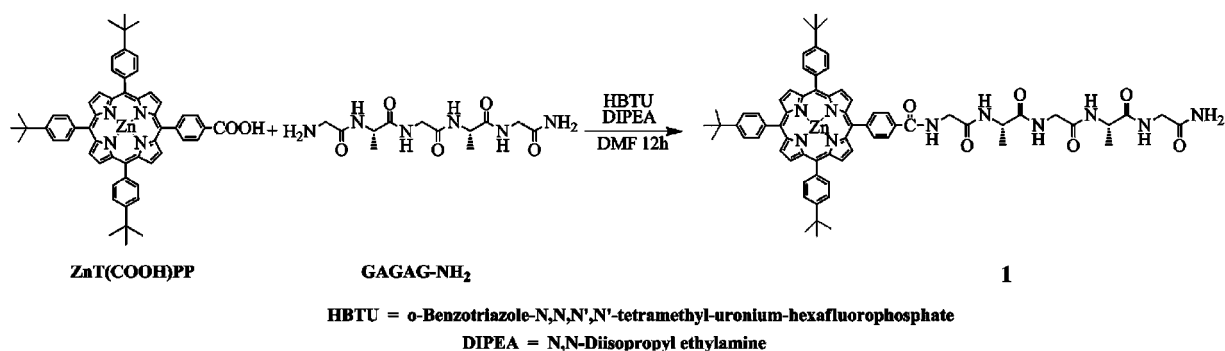
Scheme 1 Synthesis of optically active porphyrin–pentapeptide conjugate **1**.

Figure S1 (Supporting Information).† This porphyrin–pentapeptide conjugate was also characterized with a range of spectroscopic methods. The ¹H NMR spectrum of conjugate **1** was recorded in d₆-DMSO at room temperature. All the signals can be readily assigned, Figure S2 (Supporting Information).†

IR spectra

For the purpose of revealing the secondary conformation adopted by the peripheral peptide moieties, transmission Fourier transform infrared spectroscopy (FTIR) was employed to study the self-assembled nanostructures of porphyrin–pentapeptide conjugate **1** formed in THF/n-hexane (1 : 3) and THF/water (1 : 3), respectively. It is worth noting that investigation has revealed that the pronounced absorption at *ca.* 1650–1655 cm⁻¹ and a moderate strong absorption at *ca.* 1546–1550 cm⁻¹ in the IR spectra are due to the amide I band and amide II band vibrations of peptides with the α-helix secondary conformation.[12a–c] However, along with the change of the secondary conformation for peptides from α-helix to β-sheet, both the amide I band and amide II band shift to lower wave number, meanwhile a new shoulder peak appears at higher wave number.[12c–e] In the present case, as shown in Fig. 1, two absorptions at 1657 and 1542 cm⁻¹ are observed in the IR spectrum of the porphyrin–peptide conjugate **1** itself, indicating the α-helix secondary conformation of peptide chain in conjugate **1**. This is also true for the pentapeptide chain in the conjugate molecules in the aggregates of **1** formed in n-hexane due to the presence of two similar absorptions at 1661 and 1543 cm⁻¹ in the IR spectrum, Fig. 1. However, two red-shifted absorptions at 1628 and 1521 cm⁻¹, together with a new shoulder peak at 1691 cm⁻¹, are observed in the region corresponding to the amide I band and amide II band vibrations in the IR spectrum of the aggregates of **1** formed in water, suggesting the antiparallel β-sheet conformation employed by the peptide chain in the nanostructures. These results correspond well with the findings that peptide compounds usually employ α-helix and β-sheet secondary conformation in apolar and polar solvent,[11] respectively, revealing the effect of the solvent system on tuning the secondary conformation of peripheral peptide chain, and then the molecular packing mode, supramolecular chirality, and morphology of
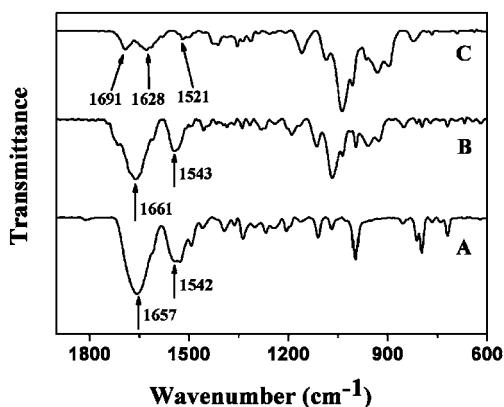
nanostructures of conjugate **1**. This is in good accordance with the CD spectroscopic and X-ray diffraction (XRD) results as detailed below.

Electronic absorption and circular dichroism (CD) spectroscopy

The electronic absorption and circular dichroism (CD) spectra of the newly prepared porphyrin–pentapeptide conjugate **1** in THF and its nano-aggregates fabricated in n-hexane and water were recorded and shown in Fig. 2, while the electronic absorption data compiled in Table S1 (Supporting Information).† In line with the 5,10,15,20-tetraphenyl-porphyrinato zinc compound ZnTPP,[13] porphyrin–peptide conjugate **1** shows a typical feature of porphyrinato zinc complex in the electronic absorption spectrum in THF, revealing the non-aggregated molecular spectroscopic nature of this compound when being dissolved in THF. As shown in Fig. 2A, the sharp absorption around 419 nm for conjugate **1** is attributed to the porphyrin Soret band, while the three typical weak absorptions at 504, 545, and 582 nm to the porphyrin Q bands. Corresponding to the electronic absorption of conjugate **1** in THF, a relatively weak positive sign in the porphyrin Soret band region was observed in the CD spectrum, Fig. 2B, indicating chiral information transfer from the chiral peripheral peptide chain to the porphyrin chromophore at the molecular level. According to the chiral exciton theory,[14] porphyrin–pentapeptide conjugate **1** is *right*-handed on the basis of the chiral information revealed by the peripheral peptide chain of conjugate **1**.

The electronic absorption spectra of the aggregates formed from conjugate **1** in THF/n-hexane (1 : 3) and THF/water (1 : 3) are also shown in Fig. 2A, respectively, which are different from that of conjugate **1** in THF. Nevertheless, significant difference also exists in the electronic absorption spectra of the aggregates formed from conjugate **1** in n-hexane and water systems, indicating different supramolecular stacking styles in these two solvent systems. As shown in Fig. 2A (red line), when conjugate
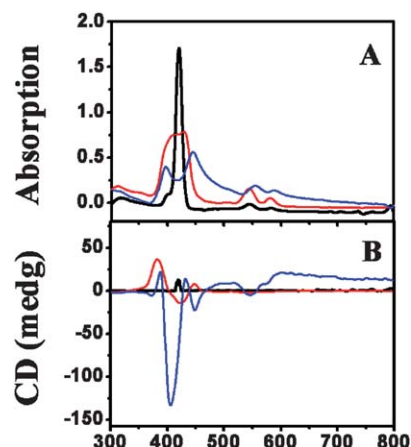

Fig. 1 IR spectra of conjugate **1** (A), its nanostructures formed in THF/n-hexane (1 : 3) (B), and its nanostructures formed in THF/water (1 : 3) (C) in the region of 600–2000 cm⁻¹ with 2 cm⁻¹ resolution.

Fig. 2 The electronic absorption spectra of conjugate **1** in THF (black line), its nanostructures fabricated from THF/n-hexane (1 : 3) dispersed in n-hexane (red line) and its nanostructures fabricated from THF/water (1 : 3) dispersed in water (blue line) (A); circular dichroism (CD) spectra of conjugate **1** in THF (black line), its nanostructures fabricated from THF/n-hexane (1 : 3) dispersed in n-hexane (red line) and its nanostructures fabricated from THF/water (1 : 3) dispersed in water (blue line) (B).

1 self-assembles into aggregates in *n*-hexane, the Soret band for conjugate **1** significantly red-shifts from 419 in THF to 439 nm with the Q bands very slightly red-shifted from 504, 545, and 582 nm in THF to 505, 546, and 583 nm in *n*-hexane. The corresponding shift for conjugate **1** in *n*-hexane was confirmed by the CD spectroscopic measurement result as detailed below. This is also true for the shift of **1** in water. However, when conjugate **1** self-assembles into aggregates in water, Fig. 2A (blue line), one absorption with the maximum red-shifted to 443 nm and a shoulder with the maximum blue-shifted to 395 nm were observed in the porphyrin Soret band region. In addition, the Q bands for conjugate **1** also red-shift from 504, 545, and 582 nm in THF to 510, 554, and 587 nm in water, Table S1 (Supporting Information).† On the basis of Kasha's theory about exciton coupling and the orientation of the transition moment in porphyrin,[15] red-shift in the main absorption bands of conjugate **1** upon aggregation both in *n*-hexane and water indicates the formation of *J* aggregates with a head-to-tail molecular stacking. However, observation of a shoulder Soret peak at 395 nm for the aggregate of **1** formed in water suggests the formation of *J* aggregates with a shorter slipping distance,[16] indicating a stronger intermolecular interaction between porphyrin chromophores.

In the CD spectra of aggregates fabricated from conjugate **1** in THF/*n*-hexane (1 : 3) and THF/water (1 : 3), Fig. 2B, one and two bisignate Cotton effects were observed in the porphyrin Soret band region, respectively. According to the semiempirical method developed by Nakanishi,[17] the given sign of coupling and the direction of dipole moment can be used to determine the chirality of stacked porphyrin chromophores in the aggregates. In general, the CD spectrum featuring a bisignate Cotton effect showing positive features at longer wavelength and negative ones at shorter wavelength indicates the *right*-handed chirality of the dipole moment (positive chirality), while conversely *left*-handed chirality (negative chirality). In the present case, the porphyrin–pentapeptide conjugate **1** shows a positive bisignated Cotton effect [424(−)/448(+)], with the crossover at 439 nm, and two negative bisignated (with the same direction of dipole moments) Cotton effects [405(−)/388(+), 448(−)/432(+)], with the crossovers at 395 and 443 nm, corresponding to the porphyrin Soret band of aggregates fabricated in *n*-hexane and water, respectively. As a consequence, the positive chirality of aggregates fabricated from conjugate **1** in *n*-hexane corresponds to a *right*-handed helical arrangement and the negative chirality of aggregates fabricated in water indicates a *left*-handed helical arrangement of corresponding molecules in a stack of porphyrin chromophores in aggregates. These results confirm the effect of the solvent system on tuning the secondary conformation of the peripheral peptide chain and in turn the porphyrin chromophore packing mode and supramolecular chirality in aggregates. At the end of this section, it is noteworthy that perhaps due to the high absorption intensity in the UV region of the porphyrin chromophore, the Cotton effect characterized the β-sheet peptide (absorption below 240 nm) was not detected in the solvent utilized.[18]

Morphology of the aggregates

The morphology of the formed aggregates was examined by transmission electronic microscopy (TEM) and scanning
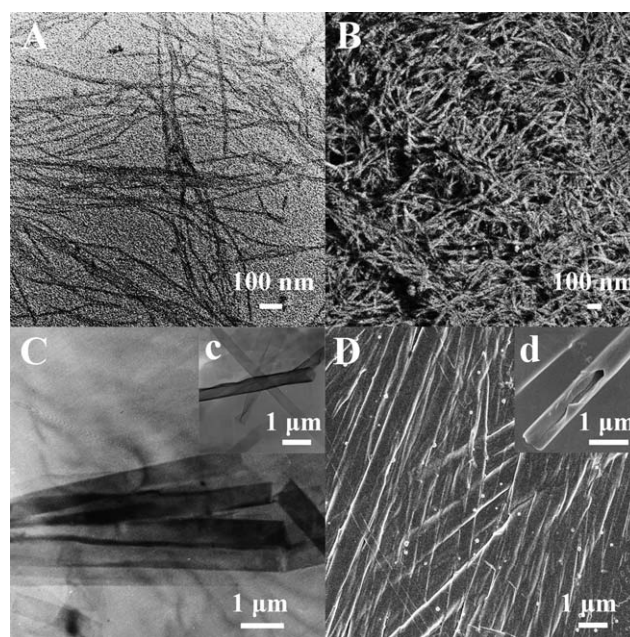

Fig. 3 Nanofibers fabricated from conjugate **1** in THF/*n*-hexane (1 : 3) observed by TEM (A) and SEM (B); nanotubes fabricated from conjugate **1** in THF/water (1 : 3) observed by TEM (C) and SEM (D); high-magnification TEM image of nanotubes fabricated from conjugate **1** in THF/water (1 : 3), indicating hollow structures (c); high-magnification SEM image of nanotubes fabricated from conjugate **1** in THF/water (1 : 3), indicating hollow structures (d).

electron microscopy (SEM), Fig. 3. Samples were prepared by casting a drop of sample solution onto a carbon-coated grid. For the purpose of investigating the influence of pentapeptide side chain on the morphology of self-assembled nanostructures, Zn[T(COOH)PP] was also fabricated into aggregates using the same method. As can be seen from Figure S3 (Supporting Information),† spherical particles with an average radius of approximately 300 nm were formed from Zn[T(COOH)PP] in THF/*n*-hexane.[19] However, introduction of a pentapeptide side chain onto the peripheral position of porphyrin ring leads to the formation of large scale of long fibrous nanostructures in THF/*n*-hexane (1 : 3), Fig. 3A and 3B. The width of these nanofibers was found in the range of 20–50 nm with the length of ten to dozens of micrometres. In line with the electronic absorption result, different morphology was observed for nanostructures formed from conjugate **1** in THF/water (1 : 3). As can be found in Fig. 3C and 3D, tubelike nanostructures with approximately 0.5–1.2 μm in width, 15–20 μm in length, and 50 nm in the wall thickness were formed from conjugate **1**. From a high-magnification TEM image in the inset of Fig. 3c, the hollow structure with the open and uneven end was clearly revealed. In addition, the high-magnification SEM image shown in the inset of Fig. 3d also confirms the hollow structure nature of these nanotubes.

Assembly mechanism

On the basis of the experimental results described above and X-ray diffraction (XRD) detailed below, the formation mechanism of nanofibers and nanotubes from conjugate **1** in *n*-hexane and water, respectively, was proposed and depicted in Fig. 4. As
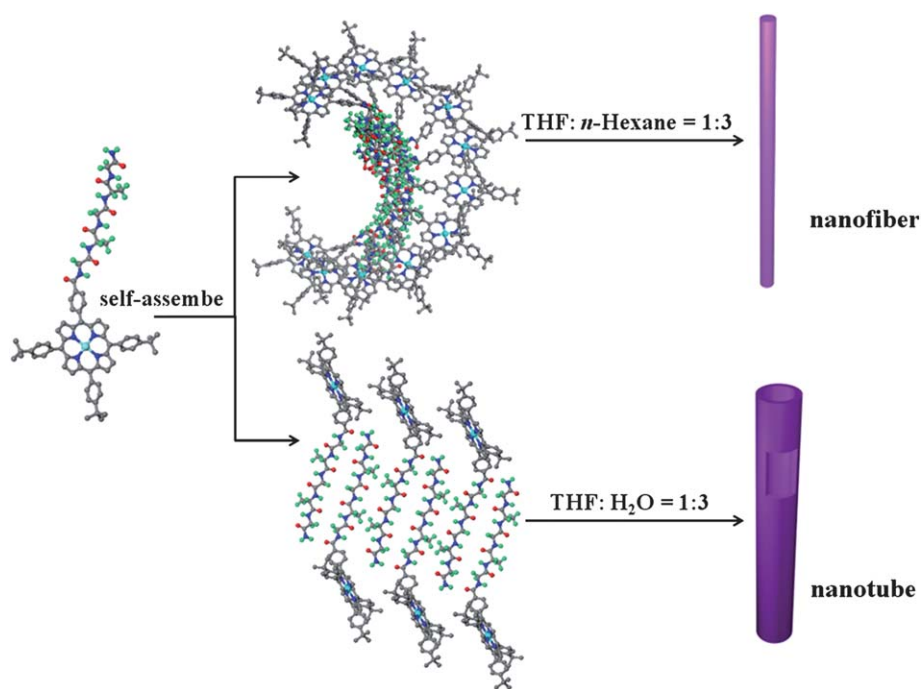
Fig. 4 Schematic illustration of a proposed mechanism for the formation of nanostructures from conjugate **1**. All the hydrogen atoms except these on the pentapeptide chains were omitted for clarity.

clearly revealed previously, peptide compounds usually employ α-helix and antiparallel β-sheet secondary conformation in apolar and polar solvent systems, respectively.[11] As a result, when the porphyrin–peptide conjugate starts to aggregate in apolar THF/n-hexane (1 : 3) systems, chiral discrimination between adjacent α-helix pentapeptide chains in cooperation with the porphyrin–porphyrin interaction in the direction parallel to the tetrapyrrole ring of neighboring conjugate **1** molecules dominates the self-assembly process, resulting in the *right*-handed helix in a stack of porphyrin chromophores. As can be seen in Fig. 5, the hydrophilic pentapeptide chain covalently linked to porphyrin ligand in conjugate **1** forms the interior of the helix, while the hydrophobic porphyrin chromophore constitutes the periphery of the helix. However, the pentapeptide chain covalently linked to the porphyrin ring adopts the antiparallel β-sheet secondary conformation in polar THF/water (1 : 3) system, which induces the formation of dimeric supramolecular bilayer structure depending on the intermolecular hydrogen bonding interaction between the pentapeptide chains of neighboring molecules of conjugate **1**, Fig. 6. The dimeric supramolecular bilayer structures further self-assemble into one-dimensional supramolecular chain depending on the hydrogen bonding interaction between dimeric building blocks, which further packs into nanotubes with *left*-handed helical arrangement in a stack of porphyrin chromophores depending on the chiral discrimination in cooperation with porphyrin–porphyrin interaction between neighboring one-dimensional supramolecular chains.[20]

X-ray diffraction patterns of the aggregates

The internal structure of self-assembled nanostructures was further investigated by X-ray diffraction (XRD) technique.

Fig. 5 and 6 also exhibit the diffraction patterns of the self-assembled nanostructures formed from conjugate **1** in THF/n-hexane (1 : 3) and THF/water (1 : 3). As can be seen in Fig. 5A, the XRD diagram of nanofibers formed from conjugate **1** in n-hexane shows a comparatively strong and narrow peak at $2\theta = 2.26°$ (corresponding to 3.91 nm) along with ten higher order diffraction peaks corresponding to $3.91/n$ nm where $n = 2, 3, 4, 6, 7, 8, 9, 11, 13$ and 14 due to the refractions from the (100) plane and its higher refractions, indicating the existence of a very regular repetition in this direction, Fig. 5. As revealed by CD spectroscopy, molecules of conjugate **1** self-assemble into *right*-handed helix in a stack of porphyrin molecules in apolar n-hexane solvent. This result, in combination with the length of a conjugate **1** (2.4 nm) obtained on the basis of geometry optimization and energy minimized molecular structure of conjugate **1** molecule using Gaussian 03 program at B3LYP/6-31G(d) level,[21] suggests that the diffraction peak at 3.91 nm should correspond to one helix diameter of a stack of conjugate **1** molecules, Fig. 5. In addition, the nanofibers present another sharp refraction at 0.32 nm in the wide angle region due to the stacking distance between neighboring porphyrin chromophores along the direction perpendicular to the porphyrin ring, in line with a previous investigation result.[22]

In the low angle range of the XRD diagram, Fig. 6A, the nanotubes formed from conjugate **1** in water show a strong refraction peak at $2\theta = 1.82°$ (4.85 nm) and two relatively weak refractions at 3.66° (2.41 nm) and 5.60° (1.58 nm), which are ascribed to the refractions from the (100), (200), and (300) planes. In addition, the XRD pattern also displays another peak at 7.16° (1.23 nm) in the low angle range and three refractions at 14.52° (0.61 nm), 21.16° (0.42 nm), and 28.98° (0.31 nm), respectively, originating from the (010) plane and its higher order refractions
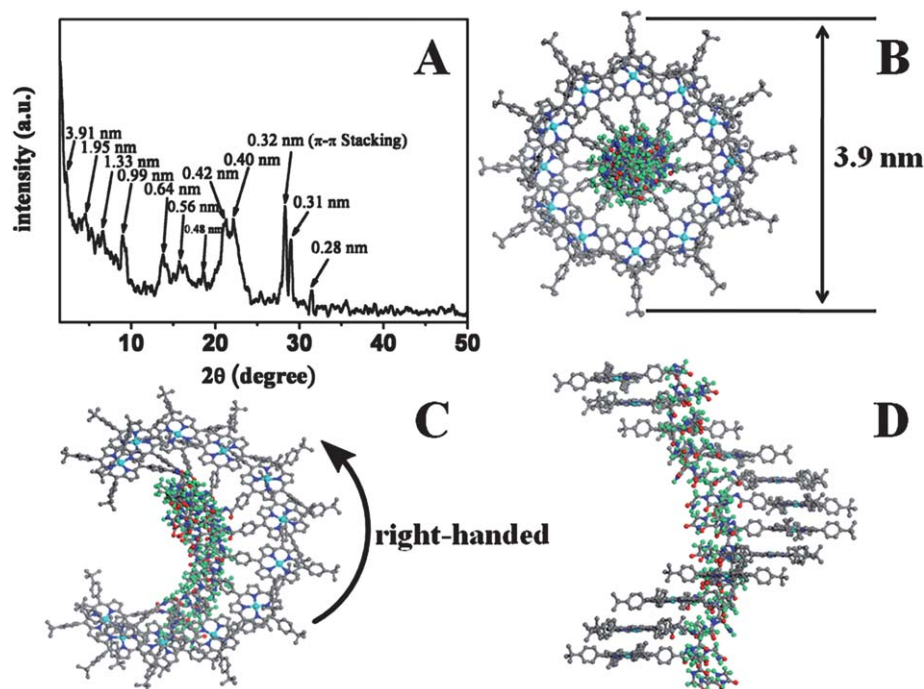
Fig. 5 XRD profile of the nanostructures fabricated from conjugate **1** in THF/*n*-hexane solution (1 : 3) (A); schematic representation of one helix in a stack of conjugate **1** molecules: top view (B), inclined view (C) and front view (D). All the hydrogen atoms except these on the pentapeptide chains were omitted for clarity.
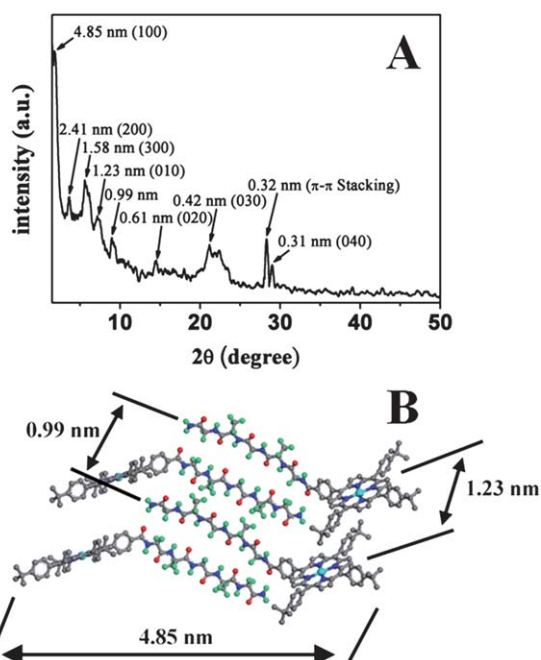

Fig. 6 XRD profile of the nanostructures fabricated from conjugate **1** in THF/water solution (1 : 3) (A); schematic representation of two dimeric supramolecular bilayer structures of the porphyrin–pentapeptide conjugate **1** (B). All the hydrogen atoms except these on the pentapeptide chains were omitted for clarity.

of (020), (030), and (040) planes. As revealed in the IR spectroscopic section, the peptide chains in the aggregates formed from conjugate **1** in water adopt antiparallel β-sheet conformation

depending on the intermolecular hydrogen bonding interaction, resulting in the formation of dimeric supramolecular bilayer structure. The evidence for this structure was also revealed from the XRD pattern by observing a refraction peak at $2\theta = 8.90°$ (0.99 nm), corresponding to the typical β-sheet inter-strand spacing between neighbouring bilayers, Fig. 6.[23] Based on these results, in combination with the size of a dimeric supramolecular bilayer structure revealed by the geometry optimization and energy minimized molecular structure of a porphyrin chromophore using Gaussian 03 program at B3LYP/6-31G(d) level[21] and a similar dimeric OPV-peptide supramolecular structure,[18] the refraction peaks at 4.85 and 1.23 nm can be ascribed to the width of a bilayer and the distance between two bilayers, Fig. 6. Similar to the X-ray diffraction of nanofibers formed from conjugate **1**, nanotubes formed from conjugate **1** also present a sharp refraction at 0.32 nm in the wide angle region, corresponding to the porphyrin–porphyrin stacking distance between two neighboring one-dimensional supramolecular chains, Figure S4 (Supporting Information).† At the end of this section, it is noteworthy that observation of the higher order refraction peaks of (100) plane for nanofibers and (100) and (010) planes for nanotubes suggests the high molecular ordering nature of these nanostructures along at least one and even two directions. This seems to correspond well with the relatively high conductivity of both nanostructures as revealed by *I–V* measurements detailed below.

I–V properties

The nanofibers and nanotubes fabricated would be promising candidates with potential applications in electronic devices. To
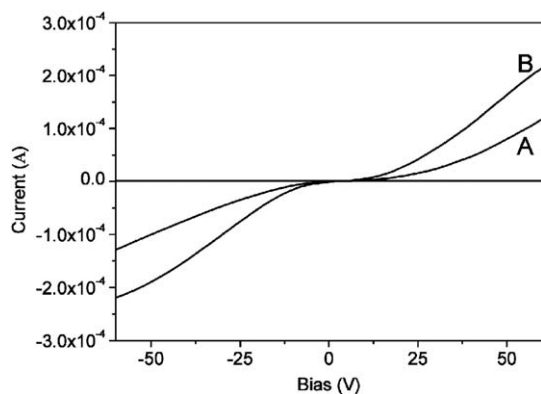
Fig. 7 *I–V* curves measured on aggregates assembled from conjugate **1** with the morphology of nanotubes (A) and nanofibers (B) from −60 V to 60 V.

demonstrate the potential of these nanostructures, these well-defined nanostructures were carefully pressed onto two Au electrodes to measure their current–voltage characteristics, Figure S5 (Supporting Information).† Fig. 7 shows the current–voltage (*I–V*) characteristics of nanofibers and nanotubes of conjugate **1**. For the devices measured, the conductivity of the nanofibers and nanotubes extracted from the quasilinear region at low bias (up to 30 V) was about 2.4×10^{-3} and 1.1×10^{-3} S m^{-1}, respectively. The quite high conductive capability of these nanostructures should be associated with the high molecular ordering nature of these nanostructures as revealed by the X-ray diffraction analysis. These nanostructures with relatively high current modulation should be useful for a wide range of electronic and sensor devices.

Conclusion

In conclusion, the self-assembly behavior of a novel optically active covalently linked porphyrin–pentapeptide conjugate **1** in different solvent systems has been comparatively investigated, revealing the effect of secondary conformation of the pentapeptide chain covalently linked to the porphyrin ring in the conjugate molecule associated with solvent system on molecular packing mode, supramolecular chirality, and morphology of nanostructures. The nanostructures fabricated were revealed to show good semiconductor feature. The present result, representing the first example of organic nanostructures self-assembled from covalently linked porphyrin–pentapeptide conjugate, will be helpful towards understanding, designing, preparing, and mimicking the structure and role of naturally occurring porphyrin–peptide conjugate systems.

Experimental section

General

N,*N*-Diisopropyl ethylamine (DIPEA, >99.5%) and *o*-benzotriazole-*N*,*N*,*N*′,*N*′-tetramethyl-uronium hexafluorophosphate (HBTU, >99%) were obtained from J&K Chemical Ltd. The GAGAG pentapeptide sequence (GAGAG–NH$_2$, >99%) was obtained from Shanghai Bootech Bioscience and Technology Co., Ltd. All other solvents were of AR quality and used as

received without further treatment. 5-(4-Carboxyphenyl)–10,15,20-tris(4-*tert*-butylphenyl)porphyrinato zinc complex Zn [T(COOH)PP] was prepared according to the published procedures.[24] Column chromatography was carried out on silica gel (Merck, Kieselgel 60, 200–300 mesh) with the indicated eluents.

Nanostructure fabrication

The self-assembled nanofibers and nanotubes fabricated from conjugate **1** were prepared by the solution mixture method according to the following procedure.[25] *n*-Hexane was injected into a solution of conjugate **1** in tetrahydrofuran (THF) (0.5 mM) to give a solution with final THF/*n*-hexane ratio of 1 : 3 (v/v) in a little flask. After the solution was allowed to equilibrate at ambient temperature for about four days, the loose aggregates were observed. These precipitates were then transferred to the carbon-coated grid by pipetting for TEM and SEM observations. The nanotubes were prepared by a similar method by injecting a solution of conjugate **1** in tetrahydrofuran (0.5 mM) to water to give a final THF/water ratio of 1 : 3 (v/v) in a little flask, respectively. The experimental results were stable and reproducible under the experimental conditions described above.

Device fabrication

Several drops of sample solution were cast onto SiO$_2$ substrate. After the solvent being evaporated, the Au electrodes were thermally evaporated onto the nanostructures by use of a shadow mask. These electrodes have width (*W*) 28.6 mm and channel length (*L*) 0.24 mm. The current–voltage characteristics were obtained with a Keithley 4200 semiconductor characterization system at room temperature in air.

Measurements

^{1}H NMR spectrum was recorded on a Bruker DPX 300 spectrometer (400 MHz) in d$_6$-DMSO using the residual solvent resonance of DMSO at 2.49 ppm relative to SiMe$_4$ as internal reference. Fourier transform infrared spectra (IR) were recorded in KBr pellets with 2 cm^{-1} resolution using a αALPHA-T spectrometer. MALDI-TOF mass spectrum was taken on a Bruker BIFLEX III ultra-high resolution Fourier transform ion cyclotron resonance (FT-ICR) mass spectrometer with α-cyano-4-hydroxycinnamic acid as matrix. Elemental analysis was performed on an Elementar Vavio El III. Transmission electron microscopic (TEM) images were measured on a JEOL-100CX II electron microscope operated at 100 kV. SEM images were obtained using a JEOL JSM-6700F field-emission scanning electron microscopy. For TEM imaging, a drop of sample solution was cast onto a carbon copper grid and flushed with methanol. For SEM imaging, Au (1–2 nm) was sputtered onto the grids to prevent charging effect and to improve the image clarity. Circular dichroism (CD) measurement and electronic absorption spectra were carried out on a JASCO J-810 spectropolarimeter and Hitachi U-4100 spectrophotometer, respectively. Low-angle X-ray diffraction (XRD) measurements were carried out on a Rigaku D/max-γB X-ray diffractometer with a Cu-Kα sealed tube (λ = 1.5406 Å) at 293 K.

Preparation of porphyrin–pentapeptide conjugate 1

Zn[T(COOH)PP] (26.71 mg, 0.03 mmol) in DMF (1 ml) was added into the DMF (0.5 ml) solution containing DIPEA (11.63 mg, 0.09 mmol) and HBTU (11.38 mg, 0.03 mmol). The mixture was reacted at room temperature under nitrogen atmosphere for ten minutes. Then, the mixture was added in a dropwise manner into the DMF (1 ml) solution containing GAGAG–NH$_2$ (9.91 mg, 0.03 mmol). After reacting at room temperature under nitrogen atmosphere for 12 h, the mixture was poured into water (80 ml). The resulting suspension was collected by filtration, washed with methanol, and purified by silica gel column chromatography. The desired conjugate **1** was eluted with 9 : 1 (v/v) chloroform/methanol as eluent, giving the product as a purple crystalline solid (14.63 mg, 40.6%). Satisfactory elemental analysis result was obtained by repeated chromatography followed by recrystallization from chloroform and methanol. ^{1}H NMR (400 MHz, d$_6$-DMSO, 25 °C): 1.24–1.33 (m, 6H, CH$_3$), 1.58 (s, 27H, *t*-butyl-CH$_3$), 3.55–4.15 (m, 6H, CH$_2$), 4.22–4.39 (m, 2H, CH), 7.06–8.31 (m, 5H, NH), 7.81–8.40 (m, 16H, Ar-H), 8.76–8.79 (t, 8H, pyrrole-H), 9.10 (s, 2H, NH$_2$).; MS: calculated for C$_{69}$H$_{72}$N$_{10}$O$_6$Zn [M]$^+$ 1200.5; Found *m/z* 1200.2. Anal. Calcd (%) for C$_{69}$H$_{72}$N$_{10}$O$_6$Zn: C 68.90, H 6.03, N 11.65; Found: C 69.06, H 6.33, N 11.54.

Acknowledgements

References

1 (a) M. Ward, *Chem. Soc. Rev.*, 1997, **26**, 365; (b) G. M. Whitesides, J. P. Mathias and C. T. Seto, *Science*, 1991, **254**, 1312; (c) J.-M. Lehn, *Science*, 2002, **295**, 2400; (d) D. Philp and J. F. Stoddart, *Angew. Chem., Int. Ed. Engl.*, 1996, **35**, 1154; (e) J. K. M. Sanders, in *Comprehensive Supramolecular Chemistry*, Vol. 9 (Eds: J. L. Atwood, J. E. E. Davies, D. D. MacNicol, F. Vögtle, D. N. Reinhoudt and J.-M. Lehn), Pergamon, New York 1996, p. 131.
2 (a) S. Bahatyrova, R. N. Frese, C. A. Siebert, J. D. Olsen, K. O. van der Werf, R. van Grondelle, R. A. Niederman, P. A. Bullough, C. Otto and C. N. Hunter, *Nature*, 2004, **430**, 1058; (b) S. Bahatyrova, R. N. Frese, K. O. van der Werf, C. Otto, C. N. Hunter and J. D. Olsen, *J. Biol. Chem.*, 2004, **279**, 21327; (c) I. W. Hwang, M. Park, T. K. Ahn, Z. S. Yoon, D. M. Ko, D. Kim, F. Ito, Y. Ishibashi, S. R. Khan, Y. Nagasawa, H. Miyasaka, C. Keda, R. Takahashi, K. Ogawa, A. Satake and Y. Kobuke, *Chem.–Eur. J.*, 2005, **11**, 3753; (d) J. Linnanto and J. E. I. Korppi-Tommola, *Phys. Chem. Chem. Phys.*, 2002, **4**, 3453.
3 (a) J. A. Shelnutt, X. Z. Song, J. G. Ma, S. L. Jia, W. Jentzen and C. J. Medforth, *Chem. Soc. Rev.*, 1998, **27**, 31; (b) A. Lombardi, F. Nastri and V. Pavone, *Chem. Rev.*, 2001, **101**, 3165; (c) J. T. Slama, H. W. Smith, C. G. Willson and H. Rapoport, *J. Am. Chem. Soc.*, 1975, **97**, 6556; (d) S. Othman, A. Le Lirzin and A. Desbois, *Biochemistry*, 1993, **32**, 9781.
4 (a) D. L. Huffman and K. S. Suslick, *Inorg. Chem.*, 2000, **39**, 5418; (b) J. R. Dunetz, C. Sandstrom, E. R. Young, P. Baker, S. A. Van Name, T. Cathopolous, R. Fairman, J. C. de Paula and K. S. Akerfeldt, *Org. Lett.*, 2005, **7**, 2559; (c) M. Aoudia and M. A. J. Rodgers, *Langmuir*, 2005, **21**, 10355; (d) D. Kuciauskas and G. A. Caputo, *J. Phys. Chem. B*, 2009, **113**, 14439; (e) D. V. Zaytsev, F. Xie, M. Mukherjee,

A. Bludin, B. Demeler, R. M. Breece, D. L. Tierney and M. Y. Ogawa, *Biomacromolecules*, 2010, **11**, 2602; (f) D. Kuciauskas, J. Riskis, G. A. Caputo and V. Gulbinas, *J. Phys. Chem. B*, 2010, **114**, 16029.
5 T. Arai, M. Inudo, T. Ishimatsu, C. Akamatsu, Y. Tokusaki, T. Sasaki and N. Nishino, *J. Org. Chem.*, 2003, **68**, 5540.
6 K. M. Kadish, K. M. Smith and R. Guilard, *The Porphyrin Handbook*, Academic Press, San Diego, 2000, Vols. 1–10; 2003, Vols. 11–20.
7 (a) B. C. Kovaric, B. Kokona, A. D. Schwab, M. A. Twomey, J. C. de Paula and R. Fairman, *J. Am. Chem. Soc.*, 2006, **128**, 4166; (b) M. Takahashi, A. Ueno and H. Mihara, *Chem.–Eur. J.*, 2000, **6**, 3196; (c) M. M. Rosenblatt, J. Y. Wang and K. S. Suslick, *Proc. Natl. Acad. Sci. U. S. A.*, 2003, **100**, 13140; (d) B. Kokona, A. M. Kim, R. C. Roden, J. P. Daniels, B. J. Pepe-Mooney, B. C. Kovaric, J. C. de Paula, K. A. Johnson and R. Fairman, *Biomacromolecules*, 2009, **10**, 1454.
8 K. A. McAllister, H. L. Zou, F. V. Cochran, G. M. Bender, A. Senes, H. C. Fry, V. Nanda, P. A. Keenan, J. D. Lear, J. G. Saven, M. J. Therien, J. K. Blasie and W. F. DeGrado, *J. Am. Chem. Soc.*, 2008, **130**, 11921.
9 C. A. Hunter and J. K. M. Sanders, *J. Am. Chem. Soc.*, 1990, **112**, 5525.
10 (a) S. Leininger, B. Olenyuk and P. J. Stang, *Chem. Rev.*, 2000, **100**, 853; (b) I. Beletskaya, V. S. Tyurin, A. Y. Tsivadze, R. Guilard and C. Stern, *Chem. Rev.*, 2009, **109**, 1659; (c) Z. Wang, C. J. Medforth and J. A. Shelnutt, *J. Am. Chem. Soc.*, 2004, **126**, 15954; (d) C. Huang, Y. Li, Y. Song, Y. Li, H. Liu and D. Zhu, *Adv. Mater.*, 2010, **22**, 3532; (e) M. Shirakawa, S. Kawano, N. Fujita, K. Sada and S. Shinkai, *J. Org. Chem.*, 2003, **68**, 5037; (f) S. Kawano, S. Tamaru, N. Fujita and S. Shinkai, *Chem.–Eur. J.*, 2004, **10**, 343; (g) R. Charvet, D. L. Jiang and T. Aida, *Chem. Commun.*, 2004, 2664; (h) H. Liu, J. Xu, Y. Li and Y. Li, *Acc. Chem. Res.*, 2010, **43**, 1496; (i) C. Huang, L. Wen, H. Liu, Y. Li, X. Liu, M. Yuan, J. Zhai, L. Jiang and D. Zhu, *Adv. Mater.*, 2009, **21**, 1721.
11 (a) F. Pattus, F. Heitz, C. Martinez, S. W. Provencher and C. Lazdunski, *Eur. J. Biochem.*, 1985, **152**, 681; (b) M. HollÓSi, A. A. Ismail, H. H. Mantsch, B. Penke, I. G. Varadi, G. K. Toth, I. LaczkÓ, I. Kurucz, Z. Nagy, G. D. Fasman and E. RajnavÓLgyi, *Eur. J. Biochem.*, 1992, **206**, 421; (c) O. Helluin, J. Breed and H. Duclohier, *Biochim. Biophys. Acta, Biomembr.*, 1996, **1279**, 1; (d) A. Villa, A. E. Mark, G. A. A. Saracino, U. Cosentino, D. Pitea, G. Moro and M. Salmona, *J. Phys. Chem. B*, 2006, **110**, 1423.
12 (a) G. Floudas, P. Papadopoulos, H. A. Klok, G. W. M. Vandermeulen and J. Rodriguez-Hernandez, *Macromolecules*, 2003, **36**, 3673; (b) P. Papadopoulos, G. Floudas, H. A. Klok, I. Schnell and T. Pakula, *Biomacromolecules*, 2004, **5**, 81; (c) T. Miyazawa and E. R. Blout, *J. Am. Chem. Soc.*, 1961, **83**, 712; (d) J. Kubelka and T. A. Keiderling, *J. Am. Chem. Soc.*, 2001, **123**, 6142; (e) A. Rosler, H. A. Klok, I. W. Hamley, V. Castelletto and O. O. Mykhaylyk, *Biomacromolecules*, 2003, **4**, 859.
13 Y. J. Aronowitz and M. Gouterman, *J. Mol. Spectrosc.*, 1977, **64**, 267.
14 (a) H. Harada and K. Nakanishi, *Circular Dichroic Spectroscopy, Exiciton Coupling in Organic Stereochemistry*, University Science Books: New York, 1983; (b) N. Kobayashi, *Chem. Commun.*, 1998, 487.
15 M. Kasha, H. R. Rawls and M. A. EI-Bayoumi, *Pure Appl. Chem.*, 1965, **11**, 371.
16 S. Okada and H. Segawa, *J. Am. Chem. Soc.*, 2003, **125**, 2792.
17 (a) N. Berova, K. Nakanishi and R. Woody, *Circular Dichroism: Princples and Applications, 2nd ed.*, Wiley-VCH: New York, 2000: pp 337–382; (b) M. Balaz, A. E. Holmes, M. Benedetti, P. C. Rodriguez, N. Berova and G. Proni, *J. Am. Chem. Soc.*, 2005, **127**, 4172; (c) V. V. Borovkov, J. M. Lintuluoto, M. Fujiki and Y. Inoue, *J. Am. Chem. Soc.*, 2000, **122**, 4403; (d) A. L. Hofacker and J. R. Parquette, *Angew. Chem., Int. Ed.*, 2005, **44**, 1053.
18 R. Matmour, I. De Cat, S. J. George, W. Adriaens, P. Leclere, P. H. H. Bomans, N. A. J. M. Sommerdijk, J. C. Gielen, P. C. M. Christianen, J. T. Heldens, J. C. M. van Hest, D. W. P. M. Lowik, S. De Feyter, E. W. Meijer and A. P. H. J. Schenning, *J. Am. Chem. Soc.*, 2008, **130**, 14576.
19 Similar spherical nanostructures were also obtained with the self-assembly of compound ZnT(COOH)PP in THF/water solution.

20 (*a*) A. Brizard, C. Aime, T. Labrot, I. Huc, D. Berthier, F. Artzner, B. Desbat and R. Oda, *J. Am. Chem. Soc.*, 2007, **129**, 3754; (*b*) D. T. Bong, T. D. Clark, J. R. Granja and M. R. Ghadiri, *Angew. Chem., Int. Ed.*, 2001, **40**, 988.

21 M. J. Frisch, G. W. Trucks, H. B. Schlegel, G. E. Scuseria, M. A. Robb, J. R. Cheeseman, J. A. Montgomery, Jr., T. Vreven, K. N. Kudin, J. C. Burant, J. M. Millam, S. S. Iyengar, J. Tomasi, V. Barone, B. Mennucci, M. Cossi, G. Scalmani, N. Rega, G. A. Petersson, H. Nakatsuji, M. Hada, M. Ehara, K. Toyota, R. Fukuda, J. Hasegawa, M. Ishida, T. Nakajima, Y. Honda, O. Kitao, H. Nakai, M. Klene, X. Li, J. E. Knox, H. P. Hratchian, J. B. Cross, C. Adamo, J. Jaramillo, R. Gomperts, R. E. Stratmann, O. Yazyev, A. J. Austin, R. Cammi, C. Pomelli, J. W. Ochterski, P. Y. Ayala, K. Morokuma, G. A. Voth, P. Salvador, J. J. Dannenberg, V. G. Zakrzewski, S. Dapprich, A. D. Daniels, M. C. Strain, O. Farkas, D. K. Malick, A. D. Rabuck, K. Raghavachari, J. B. Foresman, J. V. Ortiz, Q. Cui, A. G. Baboul, S. Clifford, J. Cioslowski, B. B. Stefanov, G. Liu, A. Liashenko, P. Piskorz, I. Komaromi, R. L. Martin, D. J. Fox, T. Keith, M. A. Al-Laham, C. Y. Peng, A. Nanayakkara, M. Challacombe, P. M. W. Gill, B. Johnson, W. Chen, M. W. Wong, C. Gonzalez, and J. A. Pople, *Gaussian 03, Revision B.05*; Gaussian, Inc.Pittsburgh, PA, 2003.

22 Y. Gao, X. Zhang, C. Ma, X. Li and J. Jiang, *J. Am. Chem. Soc.*, 2008, **130**, 17044.

23 (*a*) E. T. Powers, S. I. Yang, C. M. Lieber and J. W. Kelly, *Angew. Chem., Int. Ed.*, 2002, **41**, 127; (*b*) A. M. Squires, G. L. Devlin, S. L. Gras, A. K. Tickler, C. E. MacPhee and C. M. Dobson, *J. Am. Chem. Soc.*, 2006, **128**, 11738; (*c*) V. Castelletto, I. W. Hamley, R. A. Hule and D. Pochan, *Angew. Chem. Int. Ed.*, 2009, **48**, 2317.

24 P. Bhyrappa, C. Arunkumar and J. J. Vittal, *J. Chem. Sci.*, 2005, **117**, 139.

25 (*a*) X. C. Gong, T. Milic, C. Xu, J. D. Batteas and C. M. Drain, *J. Am. Chem. Soc.*, 2002, **124**, 14290; (*b*) K. Balakrishnan, A. Datar, R. Oitker, H. Chen, J. M. Zuo and L. Zang, *J. Am. Chem. Soc.*, 2005, **127**, 10496; (*c*) G. Lu, Y. Chen, Y. Zhang, M. Bao, Y. Bian, X. Li and J. Jiang, *J. Am. Chem. Soc.*, 2008, **130**, 11623; (*d*) W. Su, Y. X. Zhang, C. T. Zhao, X. Y. Li and J. Z. Jiang, *ChemPhysChem*, 2007, **8**, 1857; (*e*) G. Lu, X. Zhang, X. Cai and J. Jiang, *J. Mater. Chem.*, 2009, **19**, 2417.